Journal of Surgical Oncology 2008;97:445–450

Prognostic Significance of Expression of CCL5/RANTES Receptors in Patients With Gastric Cancer

HIDEKAZU SUGASAWA, MD,[1]* TAKASHI ICHIKURA, MD,[1] HIRONORI TSUJIMOTO, MD,[1] MANABU KINOSHITA, MD,[2] DAISAKU MORITA, MD,[3] SATOSHI ONO, MD,[1] KENTARO CHOCHI, MD,[1] HITOSHI TSUDA, MD,[3] SHUHJI SEKI, MD,[2] AND HIDETAKA MOCHIZUKI, MD[1]

[1]*Department of Surgery, National Defense Medical College, Tokorozawa, Saitama, Japan*
[2]*Department of Immunology and Microbiology, National Defense Medical College, Tokorozawa, Saitama, Japan*
[3]*Department of Basic Pathology, National Defense Medical College, Tokorozawa, Saitama, Japan*

Background and Objectives: The clinical significance of CCL5 has been reported in several malignancies. In this study, we examined the prognostic impact of serum CCL5 levels and the expression of CCL5 receptors on tumor cells in patients with gastric cancer.
Methods: Serum CCL5 levels in patients with gastric cancer were measured by enzyme-linked immunoabsorbent assay. Immunohistochemical staining of three chemokine receptors, CCR1, CCR3, and CCR5, which are known as CCL5 receptors, was performed in gastric cancer tissue.
Results: We found that serum CCL5 levels themselves had no impact on survival; however, higher serum CCL5 concentrations were associated with more advanced disease. Eighty-six (41%), 48 (23%), and 60 patients (28%) showed positive expression of CCR1, CCR3, and CCR5, respectively, on gastric cancer cells. Among the patients who underwent curative resection for stages II–IV disease, patients with positive CCR3 expression had significantly lower survival rates compared to those with negative CCR3 expression. Unlike CCR1, positive CCR5 expression was also associated with poorer prognosis. Multivariate analysis revealed that expression of CCR3 and/or CCR5 was an independent prognostic factor.
Conclusions: Tumor expression of CCR3 and/or CCR5 (receptors for CCL5) is associated with a lower survival rate in patients with gastric cancer.
J. Surg. Oncol. 2008;97:445–450. © 2008 Wiley-Liss, Inc.

KEY WORDS: gastric cancer; chemokine; chemokine receptor; CCR3; CCR5; CCL5/RANTES

INTRODUCTION

Initially, it was considered that chemokines played an important role as soluble factors regulating directional migration of leukocytes during inflammation; however, the potential involvement of chemokines extends beyond their roles in leukocyte recruitment. They also serve as potential sources of growth factors for tumor cells and angiogenic factors for endothelial cells [1–3].

CCL5/RANTES (Regulated on Activation, Normal T cell Expressed and Secreted) is a member of the CC chemokine family and interacts with the G protein-coupled receptors, CCR1, CCR3, and CCR5 [4]. Recently, it has been reported that CCL5 plays an important role not only in inflammatory diseases but also in cancers [5,6]. It has been demonstrated that CCL5 expression in biopsy specimens is related to tumor progression in breast cancer [7]. Kim et al. [8] demonstrated that stage IV gastric cancer patients have significantly higher serum CCL5 concentrations compared to those whose disease is in earlier stages. In a previous immunohistochemical study, we showed that CCL5 was produced not by cancer cells but by infiltrating lymphocytes in gastric cancer tissue. Furthermore, our in vitro study showed that gastric cancer cell lines, MKN45 and KATO III, expressed CCL5 receptors (CCR1, CCR3, and CCR5), and their proliferation was augmented in response to CCL5 stimulation [9]. Taken together, these findings show that CCL5 secreted by tumor-infiltrating lymphocytes may contribute to tumor progression through interaction with CCL5 receptors in gastric cancer. However, there is little information regarding the clinical significance of CCL5 and its receptors in gastric cancer patients.

In this study, we investigated the prognostic significance of serum CCL5 levels and the expression of CCL5 receptors on tumor cells in gastric cancer.

MATERIALS AND METHODS

Determination of Serum CCL5 Levels

Peripheral blood samples were obtained preoperatively from 91 gastric cancer patients who underwent surgery between 1991 and 2001 (63 men, 28 women; median age 64.2 ± 11.5 years, range 35–85 years). Blood samples were also obtained from 53 healthy volunteers (26 men, 27 women; median age 58.1 ± 9.3 years, range 40–80 years) as a control. Serum samples were frozen at −80°C until required for the assay. CCL5 concentrations were measured using a commercially available enzyme-linked immunoabsorbent assay (ELISA; Endogen, Boston, MA). Informed consent was obtained from all individuals prior to the initiation of this study.

Immunohistochemical Analysis of CCR Expressions in Gastric Cancer Tissues

Two hundred eleven patients with gastric cancer who underwent a gastrectomy between 1995 and 1997 at the National Defense Medical College Hospital (Tokorozawa, Saitama, Japan) participated in this study and underwent immunohistochemical analysis (146 men, 65 women; mean age 63.4 ± 11.8 years, range 20–86 years). Informed consent was obtained from all individuals prior to the initiation of this study.

*Correspondence to: Hidekazu Sugasawa, MD, Department of Surgery, National Defense Medical College, 3-2 Namiki, Tokorozawa, Saitama 359-8513, Japan. Fax: +81-4-2996-5205. E-mail: grd1807@ndmc.ac.jp

Received 13 October 2007; Accepted 21 December 2007
DOI 10.1002/jso.20984
Published online 22 February 2008 in Wiley InterScience (www.interscience.wiley.com).

A representative hematoxylin and eosin (H&E)-stained section was selected by microscopically reviewing routine histopathological sections, and the corresponding tissue blocks stored in the hospital were used for this study. To construct tissue microarray (TMA) blocks, a single tissue core was taken from tumor tissue of each "donor" block, and the core specimens from approximately 20 gastric cancers were transferred to a "recipient" block using a Tissue Microarrayer (Beecher Instruments, Silver Spring, MD) [10].

Immunohistochemical staining was performed for CCR1, CCR3, and CCR5 in the surgical gastric cancer specimens. After deparaffinization, the slides of 4-μm-thick TMA sections were placed in 3% H_2O_2 in phosphate buffered saline (PBS) for 10 min to quench endogenous peroxidase. To retrieve antigen, the slides were incubated using microwave in 10 mM citrate buffer for 20 min. After incubation with 2% normal swine serum (NSS; X0901; Dako Japan, Inc., Tokyo, Japan) for 10 min to block nonspecific binding, the slides were incubated with primary antibody—rabbit anti-human CCR1 polyclonal antibody (GTX70509; GeneTex, Inc., San Antonio, TX), rabbit anti-human CCR3 polyclonal antibody (GTX70769; GeneTex, Inc.), or goat anti-human CCR5 polyclonal antibody (GTX21673; GeneTex, Inc.)—diluted 1:200 in dilution buffer for 60 min at room temperature. After washing, the slides were stained using universal Dako-Cytomation LSAB + kit (K0679; Dako Japan, Inc.).

The staining for each CCR was evaluated based on the percentage of positive expression of cancer cells among all cancer cells, and the CCR expression for each patient was determined as positive when 10% or more cancer cells were stained, as reported previously [11]. CCR expression was independently evaluated by two experienced pathologists.

Statistics

Clinical stage was assigned according to the International Union Against Cancer's (UICC) TNM classification of malignant tumors [12].

Differences between groups were compared using the χ^2 test, Mann–Whitney *U*-test, or Fisher's exact method. Survival curves were generated using the Kaplan–Meier method, and the significance of the difference in survival rate was determined by the log-rank test. The Cox proportional hazard model was used for multivariate survival analysis. A *P*-value less than 0.05 was considered statistically significant. All analyses were performed using statistical software (StatView version 5.0; SAS Institute, Inc., Cary, NC).

TABLE I. Clinicopathological Features and Their Correlation With Serum CCL5 Levels in 91 Patients With Gastric Cancer

	CCL5 < 35.0 ng/ml	CCL5 ≥ 35.0 ng/ml	*P*-value
No. of cases	42	49	
Age	65.1 ± 11.5	63.5 ± 11.5	0.51
Gender			
Male	28	35	0.62
Female	14	14	
Tumor diameter (mm)	39.9 ± 21.2	56.8 ± 33.5	<0.01
Tumor depth			
T1, T2	35	29	<0.05
T3, T4	7	20	
Nodal metastasis			
Negative	26	15	<0.01
Positive	16	34	
Distant metastasis			
Negative	39	41	0.18
Positive	3	8	
TNM stage			
I, II	35	27	<0.01
III, IV	7	22	

TABLE II. Five-Year Survival Rates and Their Correlation With Serum CCL5 Levels in 91 Patients With Gastric Cancer

	5-year survival (%)		
	CCL5 < 35.0 ng/ml	CCL5 ≥ 35.0 ng/ml	*P*-value
Total patients	80.0% (n = 42)	54.3% (n = 49)	<0.05
TNM stage			
I	89.2% (n = 25)	87.5% (n = 14)	0.757
II	80.0% (n = 10)	58.7% (n = 13)	0.705
III	66.7% (n = 4)	50.0% (n = 9)	0.695
IV	33.3% (n = 3)	0% (n = 13)	0.216

RESULTS

Serum CCL5 Levels in Patients With Gastric Cancer

Ninety-one gastric cancer patients were divided into two groups according to serum CCL5 levels. A limit of 35.0 ng/ml was used, which represented the mean + 1 standard deviation (SD) of serum CCL5 concentration of the healthy volunteers. No significant differences in patient age, gender, tumor diameter, or distant metastasis were observed between the two groups (Table I). However, patients with serum CCL5 concentrations ≥35.0 ng/ml had more frequent T3 or T4 depth of invasion, and more frequent nodal involvement compared to patients with serum CCL5 concentrations <35.0 ng/ml. In addition, patients with serum CCL5 concentrations ≥35.0 ng/ml had more

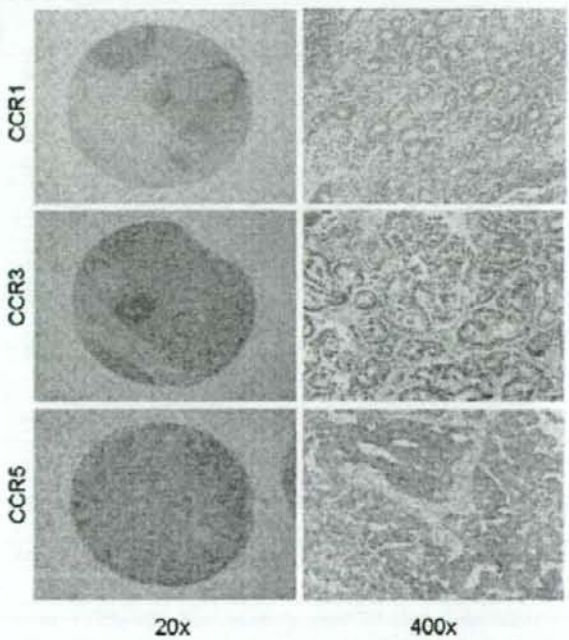

Fig. 1. Representative resected specimen demonstrating strong immunoreactivity of CCRs in gastric cancer. Each receptor is strongly positive on surface of cancer cells. Magnification: left column: 20×; right column: 400×. [Color figure can be viewed in the online issue, available at www.interscience.wiley.com.]

advanced disease, that is, stage III or stage IV, than patients with serum CCL5 concentrations <35.0 ng/ml. There was no difference in 5-year survival according to the clinical stage between patients with serum CCL5 concentrations ≥35.0 ng/ml and those with concentrations <35.0 ng/ml (Table II). In addition, multivariate survival analysis using the Cox proportional hazard model revealed that the serum CCL5 concentration had no prognostic impact in gastric cancer patients (data not shown).

Expression of CCRs in the Resected Gastric Cancer Specimen

Representative resected gastric cancer specimens demonstrating immunohistochemically positive staining for CCRs are depicted in Figure 1. The expressions of the CCRs were detected by membranous staining of the tumor cells. We observed positive expression of CCR1, CCR3, and CCR5 in the tumor cells of 86 patients (41%), 48 patients (23%), and 60 patients (28%), respectively. Sixty patients showed positive expression of only one CCR, 40 patients of two CCRs, and 18 patients of all three CCRs.

There were no significant differences in clinicopathological parameters or survival rates between 118 patients who showed positive expression for at least one of the three CCRs (CCR-positive group) and the remaining 93 patients with no expression for any of the CCRs (CCR-negative group; data not shown). Next, we analyzed survival rates according to CCR expressions in the 72 patients who had undergone a resection with curative intent for stage II, III, or IV disease, because patients with stage I tumors have extremely favorable outcomes. The CCR-positive group had a significantly poorer prognosis compared to the CCR-negative group (Fig. 2A). There were no significant differences in clinicopathological parameters between the two groups (Table III). Patients with positive CCR3 expression had significantly lower survival rates compared to patients with negative CCR3 expression. Positive CCR5 expression also had a significant deteriorating impact on survival rate, whereas CCR1 expression did not (Fig. 2B–D). We then compared survival rates according to the combination of the expressions of CCR3 and CCR5. Patients who were CCR3 positive/CCR5 negative or CCR3 negative/CCR5 positive had significantly lower survival rates than patients who were CCR3 negative/CCR5 negative. In addition, patients who were CCR3 positive/CCR5 positive had the lowest survival rate (Fig. 3). There were no differences in clinicopathological features among the three patient groups (Table IV).

Multivariate survival analysis revealed that positive expression of CCR3 and/or CCR5 was an independent prognostic factor along with TNM stage (Table V).

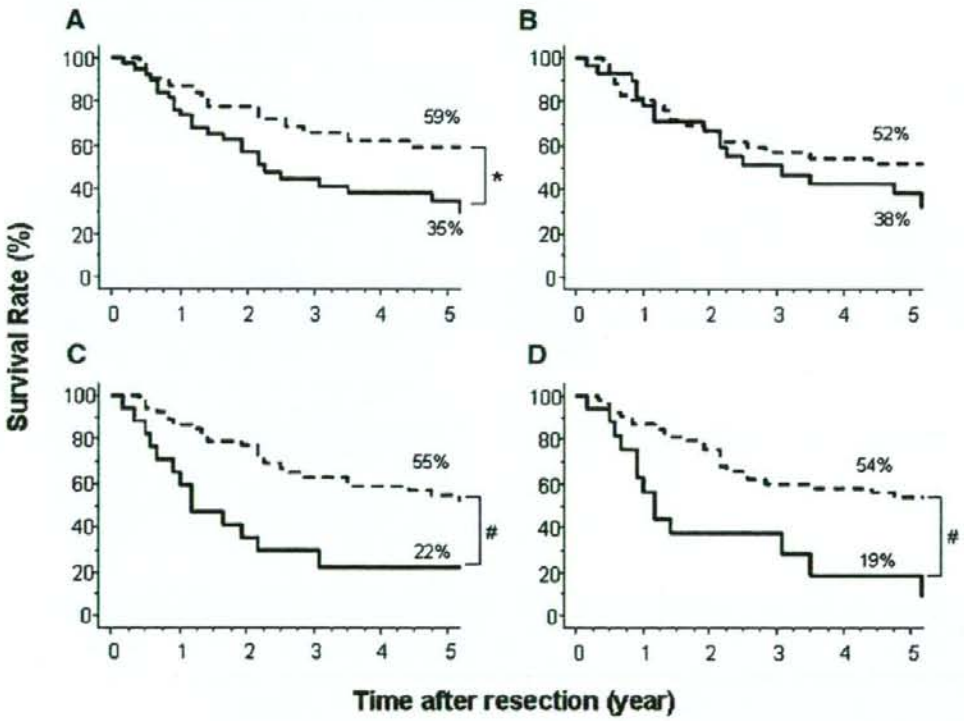

Fig. 2. Cumulative overall survival curves in patients with curative resection for stage II, III, or IV gastric cancer. **A**: Survival curve in patients with CCR-positive and CCR-negative expression. CCR-positive patients (solid line, n = 40) had significantly poor prognosis compared to CCR-negative patients (dashed line, n = 32). CCR-positive patients had at least one CCR-positive expression among three CCRs (CCR1, CCR3, and CCR5) in gastric cancer tissue. CCR-negative patients had no CCR-positive expression in gastric cancer tissue. **B**: Survival curve in patients with positive expression of CCR1 (dashed line, n = 30) or negative expression (solid line, n = 42). **C**: Survival curve in patients with positive expression of CCR3 (dashed line, n = 18) or negative expression (solid line, n = 54). **D**: Survival curve in patients with positive expression of CCR5 (dashed line, n = 18) or negative expression (solid line, n = 54). Percentage of 5-year survival rate is provided in all graphs. $^{*}P < 0.05$, $^{\#}P < 0.01$.

TABLE III. Correlation Between Clinicopathological Features and CCR Expressions in Gastric Cancer Patients Undergoing Curative Resection for Stage II, III, or IV Disease

	CCR positive	CCR negative	*P*-value
No. of cases	40	32	
Age[a]	62.9 ± 11.5	63.6 ± 8.5	0.76
Gender			
Male	31	22	0.57
Female	9	10	
Tumor diameter (mm)[a]	57.4 ± 19.5	57.7 ± 27.1	0.95
Histological type			
Intestinal type	19	15	>0.99
Diffuse type	21	17	
Lymphatic invasion			
Negative	1	0	>0.99
Positive	39	32	
Venous invasion			
Negative	2	3	0.80
Positive	38	29	
Tumor depth			
T1	1	1	0.99
T2	19	16	
T3	17	13	
T4	3	2	
Nodal metastasis			
Negative	1	1	>0.99
Positive	39	31	
Distant metastasis			
Negative	37	30	>0.99
Positive	3	2	
TNM stage			
II	14	11	0.36
III	21	13	
IV	5	8	

[a]Data are represented as mean ± SD.

TABLE IV. Clinicopathological Features of Combinations of CCR Expressions in Gastric Cancer Patients Undergoing Curative Resection for Stage II, III, or IV Disease

	Combination of CCR expressions			
	CCR3 negative and CCR5 negative	CCR3 positive or CCR5 positive	CCR3 positive and CCR5 positive	*P*-value
No. of cases	46	16	10	
Age[a]	63.4 ± 10.3	63.1 ± 7.6	62.3 ± 13.9	0.77
Gender				
Male	34	13	6	0.49
Female	12	3	4	
Tumor diameter (mm)[a]	55.0 ± 25.0	55.2 ± 14.9	63.1 ± 19.3	0.75
Histological type				
Intestinal type	19	11	4	0.15
Diffuse type	27	5	6	
Lymphatic invasion				
Negative	1	0	0	0.75
Positive	45	16	10	
Venous invasion				
Negative	4	0	1	0.46
Positive	42	16	9	
Tumor depth				
T1	1	1	0	0.52
T2	25	7	3	
T3	16	8	6	
T4	4	0	1	
Nodal metastasis				
Negative	1	1	0	0.59
Positive	45	15	10	
Distant metastasis				
Negative	42	15	10	0.61
Positive	4	1	0	
TNM stage				
II	15	8	2	0.24
III	20	7	7	
IV	11	1	1	

[a]Data are represented as mean ± SD.

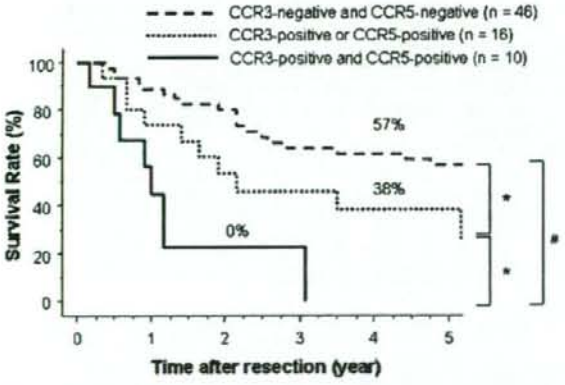

Fig. 3. Cumulative overall survival curves in gastric cancer patients according to their expression of CCR3 and/or CCR5. Patients with positive expression of either CCR3 or CCR5 expression and those with positive expression of both CCR3 and CCR5 had significantly poorer survival rates than patients with negative expression of both CCR3 and CCR5. In addition, patients with positive expression of both CCR3 and CCR5 in gastric cancer had outcomes that were significantly worse than those with positive expression of either CCR3 or CCR5. Percentage of 5-year survival rate is provided. $^{*}P < 0.05$, $^{\#}P < 0.0001$.

DISCUSSION

In this study, we found that higher serum CCL5 levels were associated with more advanced disease in patients with gastric cancer; however, serum CCL5 levels did not have a prognostic significance for any particular stage of the disease. On the other hand, the expression of

TABLE V. Multivariate Analysis of Clinicopathological Parameters for Overall Survival in Gastric Cancer Patients Undergoing Curative Resection for Stage II, III, or IV Disease

Parameter	Hazard ratio	95% CI	*P*-value
Age	1.020	0.986–1.056	0.251
Gender (male to female)	1.338	0.648–2.76	0.432
Histological type (intestinal to diffuse)	1.475	0.728–2.99	0.281
TNM stage			
Stage II	1		
Stage III	2.734	1.06–7.08	0.038
Stage IV	5.713	1.87–17.5	0.0022
Combination of CCR expressions			
CCR3 negative and CCR5 negative	1		
CCR3 positive or CCR5 positive	4.987	1.97–12.6	0.0007
CCR3 positive and CCR5 positive	6.895	2.57–18.5	0.0001

CI: confidence interval.

CCL5 receptors, particularly CCR3 and/or CCR5, was an independent prognostic indicator.

Chemokines are a group of structurally related small cytokines that commonly induce directed migration of different leukocyte populations. Based on the arrangement of the N-terminal conserved cysteine residues, chemokines are classified into four subfamilies: CC, CXC, C, and CX3C. Unlike other cytokines, chemokines interact with, and signal via, a group of seven transmembrane G protein-coupled receptors. Chemokines play essential roles in migration and homing of lymphocyte subpopulations, which express specific sets of chemokine receptors in accordance with their lineage and functional maturation [4].

There is increasing evidence that chemokines also play a role in promoting growth, survival, and metastasis of several malignancies [4,13–15]. CCL5 is a member of the CC chemokine family and a potent chemoattractant for lymphocytes as well as for monocytes, natural killer cells, and eosinophils [16]. It has been reported that high levels of serum or tissue CCL5 correlate with tumor progression and poor outcome in case of patients with several malignancies [6,7]. It has also been reported that gastric cancer patients with advanced disease have significantly higher serum CCL5 concentrations than those whose disease is in an earlier stage; this is consistent with the results of our current study [8].

Receptors for CCL5 were found to be expressed on tumor cells in several malignancies, for example, CCR1 in hepatocellular carcinoma, CCR3 in renal cell carcinoma, and CCR5 in prostate cancer [17–19]. Vaday et al. [17] demonstrated that invasion and proliferation of prostate cancer cells that expressed CCR5 were stimulated by CCL5 and that a CCR5 antagonist (TAK-779) inhibited CCL5-induced proliferation of cancer cells. Wu et al. [19] demonstrated that knockdown expression of CCR1 using micro-interfering RNA significantly inhibited the invasive ability of human hepatocellular carcinoma. Robinson et al. showed that an antagonist for both CCR1 and CCR5 could slow the growth of breast cancer cells [20]. Taken together, these findings indicate that expression of chemokine receptors for CCL5 on cancer cells may potentially contribute to promoting the invasion or progression of tumor cells through ligand binding.

We demonstrated that the expression of CCL5 receptors was correlated with clinical outcome in gastric cancer. Compared to negative expression for CCR3 and CCR5, positive expression for either receptor was associated with a significantly lower survival rate, and positive expression for both of them was associated with the lowest survival rate. Each chemokine receptor binds to multiple chemokines and vice versa, suggesting that certain redundancies exist in chemokine functions [21]. In this regard, CCL5 receptors were shared by several chemokines other than CCL5 (Table VI) [22]. However, as far as we can determine from literature, CCL5 is the only common ligand for both CCR3 and CCR5. Thus, the expression of CCR3 and CCR5 may contribute to tumor progression through their binding to CCL5.

In conclusion, our results suggest that the expression of CCRs, particularly CCR3 and/or CCR5, on cancer cells is an independent prognostic indicator for gastric cancer after curative gastrectomy. The interaction between CCL5 and its receptors may be a potential promoter of tumor progression and a possible target for treatment of gastric cancer. However, further investigation is needed to determine the mechanisms of this interaction.

TABLE VI. Ligands for CCL5/RANTES Receptors

RANTES receptor	Ligands
CCR1	CCL3/MIP-1α
	CCL5/RANTES
	CCL7/MCP-3
	CCL14/HCC-1
	CCL16/HCC-4
	CCL23/MPIF-1
CCR3	CCL5/RANTES
	CCL7/MCP-3
	CCL8/MCP-2
	CCL11/Eotaxin-1
	CCL13/MCP-4
	CCL15/HCC-2, MIP-1δ
	CCL24/MPIF-2, Eotaxin-2
	CCL26/Eotaxin-3
CCR5	CCL3/MIP-1α
	CCL4/MIP-1β
	CCL5/RANTES

Adapted from http://cytokine.medic.kumamoto-u.ac.jp/. MIP-1, macrophage inflammatory protein-1; RANTES, Regulated on Activation, Normal T cell Expressed and Secreted; MCP, macrophage chemoattractant protein; HCC, hemofiltrate CC-Chemokine; MPIF, myeloid progenitor inhibitory factor.

REFERENCES

1. Arenberg DA, Polverini PJ, Kunkel SL, et al.: The role of CXC chemokines in the regulation of angiogenesis in non-small cell lung cancer. J Leukoc Biol 1997;62:554–562.
2. Kakinuma T, Hwang ST: Chemokines, chemokine receptors, and cancer metastasis. J Leukoc Biol 2006;79:639–651.
3. Zlotnik A: Chemokines and cancer. Int J Cancer 2006;119:2026–2029.
4. Gerard C, Rollins BJ: Chemokines and disease. Nat Immunol 2001;2:108–115.
5. Duell EJ, Casella DP, Burk RD, et al.: Inflammation, genetic polymorphisms in proinflammatory genes TNF-A, RANTES, and CCR5, and risk of pancreatic adenocarcinoma. Cancer Epidemiol Biomarkers Prev 2006;15:726–731.
6. Tsukishiro S, Suzumori N, Nishikawa H, et al.: Elevated serum RANTES levels in patients with ovarian cancer correlate with the extent of the disorder. Gynecol Oncol 2006;102:542–545.
7. Niwa Y, Akamatsu H, Niwa H, et al.: Correlation of tissue and plasma RANTES levels with disease course in patients with breast or cervical cancer. Clin Cancer Res 2001;7:285–289.
8. Kim HK, Song KS, Park YS, et al.: Elevated levels of circulating platelet microparticles, VEGF, IL-6 and RANTES in patients with gastric cancer: Possible role of a metastasis predictor. Eur J Cancer 2003;39:184–191.
9. Sugasawa H, Ichikura T, Kinoshita M, et al.: Gastric cancer cells exploit CD4+ cell-derived CCL5 for their growth and prevention of CD8+ cell-involved tumor elimination. Int J Cancer 2008 (in press).
10. Shinto E, Tsuda H, Ueno H, et al.: Prognostic implication of laminin-5 gamma 2 chain expression in the invasive front of colorectal cancers, disclosed by area-specific four-point tissue microarrays. Lab Invest 2005;85:257–266.
11. Ueda S, Hatsuse K, Tsuda H, et al.: Potential crosstalk between insulin-like growth factor receptor type 1 and epidermal growth factor receptor in progression and metastasis of pancreatic cancer. Mod Pathol 2006;19:788–796.
12. Sobin LH, Fleming ID: TNM Classification of Malignant Tumors, fifth edition (1997). Union Internationale Contre le Cancer and the American Joint Committee on Cancer. Cancer 1997;80:1803–1804.
13. Muller A, Homey B, Soto H, et al.: Involvement of chemokine receptors in breast cancer metastasis. Nature 2001;410:50–56.
14. Mashino K, Sadanaga N, Yamaguchi H, et al.: Expression of chemokine receptor CCR7 is associated with lymph node metastasis of gastric carcinoma. Cancer Res 2002;62:2937–2941.
15. Yasumoto K, Koizumi K, Kawashima A, et al.: Role of the CXCL12/CXCR4 axis in peritoneal carcinomatosis of gastric cancer. Cancer Res 2006;66:2181–2187.
16. Schall TJ, Bacon KB: Chemokines, leukocyte trafficking, and inflammation. Curr Opin Immunol 1994;6:865–873.

17. Vaday GG, Peehl DM, Kadam PA, et al.: Expression of CCL5 (RANTES) and CCR5 in prostate cancer. Prostate 2006;66:124–134.
18. Johrer K, Zelle-Rieser C, Perathoner A, et al.: Up-regulation of functional chemokine receptor CCR3 in human renal cell carcinoma. Clin Cancer Res 2005;11:2459–2465.
19. Wu X, Fan J, Wang X, et al.: Downregulation of CCR1 inhibits human hepatocellular carcinoma cell invasion. Biochem Biophys Res Commun 2007;355:866–871.
20. Robinson SC, Scott KA, Wilson JL, et al.: A chemokine receptor antagonist inhibits experimental breast tumor growth. Cancer Res 2003;63:8360–8365.
21. Slettenaar VI, Wilson JL: The chemokine network: A target in cancer biology? Adv Drug Deliv Rev 2006.
22. Zlotnik A, Yoshie O: Chemokines: A new classification system and their role in immunity. Immunity 2000;12:121–127.

Jpn J Clin Oncol 2008;38(4)250–258
doi:10.1093/jjco/hyn019

Clinicopathological and Prognostic Relevance of Uptake Level using ^{18}F-fluorodeoxyglucose Positron Emission Tomography/ Computed Tomography Fusion Imaging (^{18}F-FDG PET/CT) in Primary Breast Cancer

Shigeto Ueda[1], Hitoshi Tsuda[2], Hideki Asakawa[1], Takashi Shigekawa[3], Kazuhiko Fukatsu[4], Nobuo Kondo[5], Mikio Yamamoto[5], Yukihiro Hama[6], Katsumi Tamura[6], Jiro Ishida[6], Yoshiyuki Abe[6] and Hidetaka Mochizuki[1]

[1]Department of Surgery, National Defense Medical College, Tokorozawa, Saitama, [2]Department of Basic Pathology, National Defense Medical College, Tokorozawa, Saitama, [3]Department of Breast Oncology, International Medical Center, Saitama Medical University, Hidaka, Saitama, Japan, [4]Department of Basic Traumatology, National Defense Medical College, Tokorozawa, Saitama, [5]Department of Biochemistry, National Defense Medical College, Tokorozawa, Saitama and [6]Tokorozawa PET diagnostic Imaging clinic, Tokorozawa, Saitama

Received January 13, 2008; accepted February 21, 2008

Objective: Using integrated ^{18}F-fluorodeoxyglucose positron emission tomography/computed tomography fusion imaging (^{18}F-FDG PET/CT), the clinical significance of ^{18}F-FDG uptake was evaluated in patients with primary breast cancer.

Methods: Clinicopathological correlation with the level of maximum standardized uptake values (SUV) 60 min obtained from preoperative ^{18}F-FDG PET/CT were examined in 152 patients with primary breast cancer. The prognostic impact of the level of SUV was explored using simulated prognosis derived from computed program Adjuvant! in 136 (89%) patients with invasive ductal carcinoma (IDC).

Results: High SUV level was significantly correlated with tumor invasive size ($\leq$2 cm) ($P < 0.0001$), higher score of nuclear grade ($P < 0.0001$), nuclear atypia ($P < 0.0001$) and mitosis counts ($P < 0.0001$), negative hormone receptor status ($P = 0.001$), high score of c-erbB-2 expression ($P = 0.006$), lymph node metastasis ($P = 0.002$), and IDC in comparison with invasive lobular carcinoma ($P = 0.004$). Multivariate analyses showed tumor invasive size, nuclear grade and estrogen receptor negativity were significantly correlated with SUV in primary breast cancer ($P < 0.0001, < 0.0001$, and < 0.012, respectively), and nuclear grade was significantly correlated with SUV in tumors of invasive size 2 cm or less ($P < 0.0001$). Tumors with high SUV (cutoff value 4.0) showed higher relapse and mortality rate compared to those with low SUV ($P < 0.0001$).

Conclusions: High uptake of ^{18}F-FDG would be predictive of poor prognosis in patients with primary breast cancer, and aggressive features of cancer cells in patients with early breast cancer. ^{18}F-FDG PET/CT could be a useful tool to pretherapeutically predict biological characteristics and baseline risk of breast cancer.

Key words: breast cancer – ^{18}F-FDG – PET/CT – SUV – prognosis

INTRODUCTION

^{18}F-fluorodeoxyglucose positron emission tomography (^{18}F-FDG PET), a modality of imaging glucose metabolism in cancer cells, is a new approach for staging of primary cancer and detection of distant metastasis (1–3).

For reprints and all correspondence: Hitoshi Tsuda, Department of Basic Pathology, National Defense Medical College, 3-2 Namiki, Tokorozawa, Saitama 359-8513, Japan. E-mail: htsuda@ndmc.ac.jp

Breast cancer cells overexpress glucose transporter at the membrane and the level of active hexokinase in their cytoplasm is increased compared with adjacent normal tissues. The uptake of ^{18}F-FDG by breast cancer cells is reported biologically to reflect their glucose hypermetabolism (4,5). Some studies suggested that the level of ^{18}F-FDG uptake in breast cancers is significantly correlated with tumor size, higher histological grade, Ki-67 labeling index, the number of mitotic figures and abrogation of the p53. Therefore,

primary breast cancers with higher levels of ^{18}F-FDG uptake are considered to have more aggressive potential than those with low ^{18}F-FDG uptake (6,7).

Recently, the integrated ^{18}F-FDG PET/Computed tomography fusion imaging (^{18}F-FDG PET/CT) has been shown to be able to visualize anatomical localization of the hypermetabolic cancer lesions more accurately than ^{18}F-FDG PET only. Therefore, the ^{18}F-FDG PET/CT would be more informative for pre-therapeutic staging of the entire body and for the evaluation of proliferation activity of the tumors than a single examination of ^{18}F-FDG PET (8).

To date, the most significant prognostic parameters of breast cancer are axillary nodal status, size of the primary tumor, c-erbB-2 (HER2/neu), estrogen receptor (ER) and progesterone receptor (PgR). On the other hand, a definite conclusion remains to be reached concerning the prognostic relevance of the level of ^{18}F-FDG uptake in breast cancer.

In the present study, we investigate the clinicopathological implications of the level of standardized uptake values (SUV) obtained from preoperative ^{18}F-FDG-PET/CT imaging in 152 patients with newly diagnosed primary breast cancer in our institute. We assessed levels of ^{18}F-FDG uptake to breast cancer using maximum SUV obtained 60 min later after injection of ^{18}F-FDG. In addition, we examined the prognostic relevance of the level of ^{18}F-FDG uptake using computed program Adjuvant!.

PATIENTS AND METHODS

Eligible Patients

Between April 2005 and March 2007, ^{18}F-FDG PET/CT scans were performed for 152 patients to determine clinical staging of breast cancer before initial therapy. Primary breast cancer was histopathologically diagnosed with fine needle aspiration cytology and/or core needle biopsy (CNB). Patients who did not have the evidence of distant metastatic spread using X-ray, ultrasonography, or ^{18}F-FDG PET/CT were eligible for operable candidates of primary breast cancer. Patients who were pregnant, who were taken history of insulin-depended diabetes mellitus from clinical notes, or who had previously received treatment to breast cancer were excluded from indication for ^{18}F-FDG PET/CT. All patients underwent surgery within 4 weeks after ^{18}F-FDG PET/CT examination.

The study was carried out in accordance with the ethical principles of the Declaration of Helsinki and was approved by the institutional review board in our medical school. Informed consent was obtained from all patients with regard to ^{18}F-FDG PET/CT examination.

^{18}F-FDG PET/CT and Quantification of ^{18}F-FDG uptake in Primary Breast Cancer

All patients received ^{18}F-FDG PET/CT scans (Biograph LSO Emotion, Siemens) at Tokorozawa PET Diagnostic Imaging Clinic (Tokorozawa, Japan).

Patients were fasted at least 4 h before ^{18}F-FDG PET study. One hour after intravenous administration of 3.7 Mbq/kg ^{18}F-FDG, a transmission scan using CT for attenuation correction and anatomical imaging was acquired for 90 s. IV contrast was not administered to patients for the CT portion of the ^{18}F-FDG PET/CT.

Back projection image was obtained after Gaussian filter was applied. The spatial resolution of the reconstructed images was 6.0–7.0 mm in cranio-caudal, 6.3–7.1 mm in right–left and 6.3–7.1 mm in anterior–posterior directions.

A regions of interest (ROI) was placed in the primary lesion (Fig. 1), including the highest uptake area (circle ROI, 2 cm in diameter) and SUV maximum in the ROI was calculated. The SUV was calculated using the following formula: SUV = activity in region of interest (MBq/ml)/injected dose (MBq/kg body weight).

SUV is decay-corrected tissue activity divided by the injected dose per patient body.

Surgery

A total of 152 patients received mastectomy or breast conserving surgery with sentinel node biopsy or axillary dissection. In all patients, primary systemic therapy was not performed before surgery. Sentinel node biopsy was performed by the procedure written previously (9).

Patient Characteristics

This study consisted of 152 female patients (age range 34–81 years, mean 54 years). Patients included 3 (2%) patients with Stage 0, 46 (30%) patients with Stage I, 98 (64%) patients with Stage II, 5 (4%) patients with Stage III (Table 1). Averaged SUV stratified by pathological stages consisted 3.1 (±2.1 SD) in Stage 0, 3.3 (±2.5 SD) in Stage I, 5.6 (±3.7 SD) in Stage II and 5.7 (±4.3 SD) in Stage III (Table 2). For the purposes of this study, the following characteristics were recorded from patients' clinical charts. Primary tumor features included age, sizes of tumor invasive size (cm), histological types (invasive ductal carcinoma (IDC), invasive lobular carcinoma (ILC), ductal carcinoma *in situ* (DCIS), mucinous carcinoma, and apocrine carcinoma), nuclear grade with nuclear atypia score and mitotic count score, axillary lymph node involvement, ER status, PgR status and c-erbB-2 status (Table 1). Tumor invasive size was estimated by measuring a maximum diameter of tumor invasive component (cm).

Immunohistochemistry

Formalin-fixed tumor samples obtained from surgery were routinely fixed with formalin, embedded in paraffin, cut into 4 μm-thick sections and subjected to immunohistochemistry. The expressions of ER and PgR, and c-erbB-2 were analysed immunohistochemically using specific primary antibody (Dako, Grostrup, Denmark) as previously written in our reports (10).

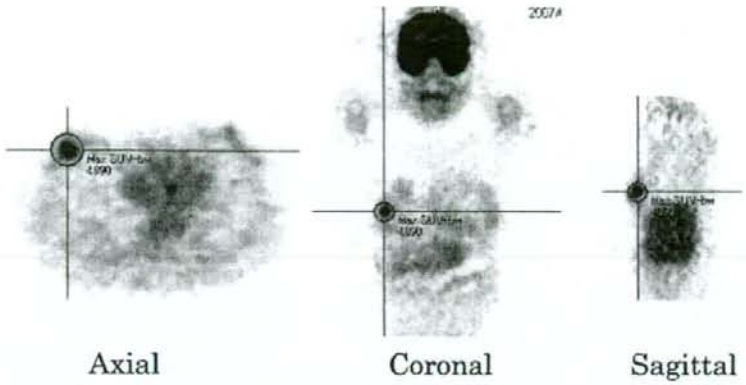

Figure 1. For semiquantitative of ^{18}F-FDG uptake, the region of interest (ROI) was placed in the primary lesion, including the highest uptake area (circular ROI, 2 cm in diameter), and maximum standardized update values (SUV) in the ROI was calculated. SUV is decay-corrected tissue activity divided by the injected dose per patient body. Representative axial, coronal and sagittal ROIs were shown in this figure. The spatial resolution of the reconstructed images was 6.0–7.0 mm in cranio-caudal, 6.3–7.1 mm in right-left and 6.3–7.1 mm in anterior-posterior directions.

Scoring System of Nuclear Grade

Nuclear grade of IDC was given according to General Rules for Clinical and Pathological Recording of Breast Cancer, 15th edition by two pathologists always including one who is experienced in breast pathology (HT) (11). Nuclear grade was given by the sum of the nuclear atypia score and the mitosis counts score. Nuclear atypia score was defined as following; Score 1: Nuclei were relatively uniform in size and shape, and chromatin was inconspicuous. Score 2: Intermediate between 1 and 3. Score 3: There were considerable variations in size and shape of nuclei and the increase and unevenness of chromatin, sometimes having giant nucleoli. After selecting the area in which mitoses were the most abundant on low to intermediate magnifications, the mitotic figures were counted on a high magnification. Mitotic count score was defined as following; Score 1: 0–4 mitoses, Score 2: 5–10 mitoses, Score 3: more than 10 mitoses per 10 high power fields using eyepieces of 20 mm field of view (40× Objective).

Simulated Prognosis Derived from Ajuvant! And SUV in Breast Cancer

The computed program Adjuvant! is an assistant tool for making decisions of adjuvant therapies for women with breast cancer (http://www.adjuvantonline.com). We used the computed program Adjuvant! to simulate the prognostic significance of the level of SUV in tumor. For the entries of information including age, menopausal status, tumor size, number of positive axillary nodes and ER status, baseline prognostic estimates are given by each patient. Physical conditions of all patients were in good health. Estimated incidences of recurrence and mortality 10 years after surgical therapy was computed by this program (12). And we compared estimated prognosis in baseline risk between high and low SUV groups by showing bow and whisker plot.

Univariate Analyses According to Clinicopathological Parameters and Prognosis

The correlations between levels of SUV and clinicopathological parameters were evaluated using the Mann–Whitney *U*-test and the Kruskal–Wallis test. A value of $P < 0.05$ was defined to be statistically significant. All statistic analyses were performed using Statview5.0 software (SAS Institute Inc.). The *t*-value is calculated by the formula: $t\text{-value} = (Y_A - Y_B)/s\sqrt{1/NA + 1/NB}$, where Y_A, the mean percentage of prognosis in low SUV group; Y_B, the mean percentage of prognosis in high SUV group; s, standard deviation; NA, sample size of low SUV group; NB, sample size of high SUV group. *T*-statistics determine whether prognosis rates of the low SUV group and the high SUV group differ significantly. According to the analysis, an explanatory factor showing an absolute *t*-value, which is more than 2, is significantly correlated with dependent variables.

Multivariate Analysis

Multiple regression analysis was performed to select independent clinicopathological variables associated with SUV for all 152 patients with primary breast cancer and for 78 patients having primary breast cancer with tumor invasive size 2 cm or less. Multivariate models were correlated using variables with a $P < 0.05$ in the univariate analyses. Variables in these models were included tumor invasive size, nuclear grade, ER, HER2 and nodal status. Histology was not entered in the models because a majority of cases were IDC. SUV and tumor invasive size was analysed as continuous variables, nuclear grade was categorized as grade 1 or 2

Table 1. Patient characteristics

Variables	Number = 152	(%)
Age		
[range]	[34–81]	
<45	29	(19)
45≤	123	(81)
Tumor invasive size (cm)		
≤2	78	(51)
2<	74	(49)
Histology		
DCIS	3	(2)
IDC	136	(89)
ILC	9	(6)
Apocrine	2	(1)
Mucinous	2	(1)
Nuclear grade		
1	43	(28)
2	36	(24)
3	60	(39)
Not graded	13	(9)
Nuclear atypia score		
1	32	(21)
2	71	(47)
3	36	(24)
Not graded	13	(9)
Mitotic count score		
<5	61	(40)
5 to 10	33	(22)
≥11	58	(38)
Nodal metastasis		
negative	99	(65)
positive	53	(35)
Estrogen receptor (ER)		
10%>	33	(22)
10%≤	119	(78)
Progesterone receptor (PgR)		
10%>	50	(33)
10%≤	102	(67)
c-erbB-2 (HER2)		
0	40	(26)
1+	74	(49)
2+	17	(11)
3+	14	(9)
unknown	7	(5)
Approach to primary tumor		
Lunpectomy	62	(41)
Mastectomy	90	(59)
Primary axillary approach		
Ax dissection	75	(49)
SLNB	77	(51)
Pathological stage		
0	3	(2)
I	46	(30)
II	98	(65)
III	5	(3)
Standardized update value (SUV)		
[range]	[0.94–17.8]	
≤4.0	83	(55)
4.0<	69	(45)

DCIS, ductal carcinoma *in situ*; IDC, invasive ducta carcinoma; ILC, invasive lobular carcinoma; Ax, axillary; SLNB, sentinel node biopsy.

versus grade 3, ER was categorized as negative versus positive, HER2 was categorized as scores 0 or 1+ versus score 2+ or 3+, and nodal status was categorized as nodal metastasis positive versus negative. All statistic analyses were performed using Statview5.0 software (SAS Institute Inc.).

RESULTS

Patient Characteristics

The clinicopathological features of the 152 patients are listed in Table 1. One hundred and thirty-six tumors (89%) were IDC, nine tumors (6%) were ILC and three tumors (2%) were DCIS. Other special subtypes included 2 (1%) apocrine carcinoma and 2 (1%) mucinous carcinoma.

Comparison Between SUV and Clinicopathological Parameters

In 152 primary breast cancers, the average level of SUV was 5.0 (Standard deviation, SD. 3.5). The correlations of the level of SUV with clinicopathological parameters were presented in Table 2.

The levels of SUV were significantly different between the patients tumor groups of 2 cm or less and greater than 2 cm, respectively ($P < 0.0001$).

The mean level of SUV was significantly lower in ILC than IDC ($P = 0.004$). Differences in the uptake level were not significantly between IDC and DCIS and between IDC

Table 2. Correlations between clinicopathological parameters and the levels of SUV

Variables	Comparision	SUV (Mean ± SD)	*P* value
Age (year)	<45	5.0 ± 3.3	0.45*
	45≤	4.4 ± 3.4	
Tumor invasive size (cm)	≤2	3.3 ± 2.7	<0.0001*
	2<	5.8 ± 3.6	
Histology	DCIS	3.1 ± 2.1	
	IDC	4.8 ± 3.5	0.004*
	ILC	1.4 ± 1.5	
	Apocrine	4.3 ± 3.2	
	Mucinous	3.0 ± 0.1	
Nuclear Grade	Grade 1	3.4 ± 3.4	<0.0001†
	Grade 2	4.0 ± 2.3	
	Grade 3	6.3 ± 3.5	
Nuclear atypia score	1	2.9 ± 3.0	<0.0001†
	2	4.8 ± 2.4	
	3	6.2 ± 3.5	
Mitotic counts score	0–4	2.7 ± 2.2	<0.0001†
	5–10	4.8 ± 3.2	
	11≤	5.9 ± 3.7	
Estrogen receptor (ER)	ER+	4.0 ± 3.0	0.001*
	ER−	6.4 ± 4.1	
Progesterone receptor (PgR)	PgR+	4.1 ± 2.9	0.04*
	PgR−	5.4 ± 4.2	
Combined hormone receptors	ER+ and/or PgR+	4.0 ± 3.0	0.001*
	ER− and PgR−	6.4 ± 4.1	
c-erbB-2 (HER2)	0 and 1+	4.0 ± 3.1	0.006*
	2+ and 3+	6.2 ± 4.2	
Nodal metastasis	Negative	3.9 ± 3.1	0.002*
	Positive	5.7 ± 3.7	
Pathological stage	0	3.1 ± 2.1	0.006†
	I	3.3 ± 2.5	
	II	5.6 ± 3.7	
	III	5.7 ± 4.3	

*Mann-Whitney *U*-test, †Kruskal-Wallis test.
Abbreviations used are same as those used in Table 1.

and other special subtypes, although the mean SUV level in DCIS was relatively low.

With regard to tumor nuclear grade and its components, the mean level of SUV was significantly different among the tumor groups of Grade 1, Grade 2 and Grade 3 ($P < 0.0001$). The mean level of SUV elevated on stepwise manner in accordance with increase in nuclear atypia score and mitotic count (each, $P < 0.0001$).

Table 3. Multiple regression analysis for 152 patients with primary breast cancer

Variables	*t* value	*P* value	*R*, Adjusted R^2
Tumr invasive size	4.52	<0.0001	0.85
Grade	4.91	<0.0001	0.72
ER	2.55	0.012	
HER2	0.93	0.36	
Nodal metastasis	0.67	0.5	

Between ER-positive group (10%≤) and ER-negative group (10%>), the mean levels of SUV of ER-negative group was significantly higher than that of ER-positive group ($P = 0.001$). Between PgR-positive (10%≤) and PgR-negative groups (10%>), the mean SUV of the PgR-negative groups was significantly higher than that of PgR-positive groups ($P = 0.04$).

With regard to combined hormone receptors status, between the tumor group of ER-positive and/or PgR-positive and of ER-negative and PgR-negative in combined receptors, the mean levels of SUV of the latter were also higher than that of the former ($P = 0.001$).

With regard to c-erbB-2 status, the mean level of SUV was higher in the tumor groups of scores 2+ and 3+ than in the tumor groups of scores 0 and 1+ ($P = 0.006$).

With regard to lymph nodal status, the mean level of SUV was higher in the tumor group with metastatic lymph nodes than in the group without metastatic lymph nodes (3.9 ± 3.1 SD) ($P = 0.002$).

Tumor invasive size ($P < 0.0001$), nuclear grade ($P < 0.0001$) and ER status ($P = 0.012$) independently influenced on the stats of SUV (4.0 or higher versus <4.0) in a multiple regression model for 152 patients (Table 3). The correlation coefficient (R^2) of combination of three parameters with SUV was 0.72. In a multiple regression model for 78 patients having primary breast cancer with tumor invasive size 2 cm or less, nuclear grade only was the independent factor that influenced on the status of SUV ($P < 0.0001$). The correlation coefficient (R^2) of nuclear grade with SUV was 0.7 (Table 4).

Patients' Prognosis and Cutoff Value of SUV

We performed a simulation of prognostic baseline risk according to 136 patients with IDC. Sixteen patients with tumors of special types including ILC, mucinous carcinoma and apocrine carcinoma were excluded from the evaluation.

The prognostic impact of the level of SUV in tumors was explored for various cutoff values in 136 IDCs. Cases were defined into two groups by six tentative thresholds (2.0, 3.0, 3.5, 4.0, 4.5 and 5.0) of SUV. Table 5 shows the number of patients who exceeded the threshold (high SUV group) and whose SUVs were the value of threshold or less (low SUV

Table 4. Multiple regression analysis for 78 patients with tumor size of 2.0 cm or less

Variables	*t* value	*P* value	*R*, adjasted R^2
Tumr invasive size	1.66	0.1	0.84
Grade	3.84	0.003	0.7
ER	0.49	0.63	
HER2	0.76	0.45	
Nodal metastasis	0.45	0.65	

group), estimated incidence of relapse and mortality after 10 years, *t*-value and *P* value were compared.

The *P* value between tentative low and high SUV groups increased in accordance with elevation of cutoff SUV up to the value of 3.0. However, the *P* values between the low and high SUV groups did not differ ($P < 0.0001$) when a cutoff value between the two SUV groups exceeded 3.0. All of absolute *t*-values between tentative low and high SUV groups were more than 2.0 and when the cutoff SUV was 4.0, the absolute *t*-value was maximal. Therefore, we defined cutoff value between the low SUV group and the high SUV group as 4.0.

On a prognostic evaluations by computed program Adjuvant!, patients with the low SUV group (4.0 or less) had tendency of lower 10-year relapse rate and 10-year mortality than the high SUV group (more than 4.0).

Sixty-five patients with low SUV tumors were estimated to show a 29.5% (±18.2 SD) and a 13.4% (±17.1 SD) of 10-year recurrence rate and mortality, respectively, whereas 71 patients with high SUV tumors were estimated to show a 51.0% (±23.2 SD) and a 33.3% (±23.4 SD) of 10-year recurrence rate and mortality, respectively. Both of estimated relapse rate and mortality differed significantly between the high SUV group and the low SUV group ($P < 0.0001$, each).

Tumor Characteristics in the Cases that Showed Discrepancy Between SUV and Prognosis Simulated by Computed Program Adjuvant!

Table 6 shows clinicopathological characteristics of 12 patients with discrepancy between their estimated prognosis and SUV uptake values of primary tumors. Four cases (L1–L4) were estimated to be poor prognosis despite being categorized in the low SUV group (SUV 4.0 or less). In the four patients in the low SUV group, the SUV averaged 2.6 (2.14–2.82) and size of tumor invasion averaged 5.3 cm. All of the four patients had lymph node involvement in their axilla.

Other eight cases (H1–H8) were estimated to be better prognosis despite being categorized in the high SUV group (SUV higher than 4.0). In the eight patients in the high SUV group, the SUV averaged 6.8 (4.42–14.7) and size of tumor invasion averaged 1.3 cm. All patients had no metastastic foci in their axillary lymph nodes.

DISCUSSION

In the univariate analyses, we clearly demonstrated high SUV level detected with ^{18}F-FDG PET/CT was correlated with bigger invasion size of tumor, higher nuclear grade, higher scores of nuclear atypia and mitosis counts, negative hormone receptor status, high score of c-erbB-2 expression, lymph node metastasis and IDC in comparison with ILC.

Above all, mean level of SUV was lower than 4.0 in the groups of diameter of tumor invasion with 2.0 cm or less. DCIS, ILC, mucinous carcinoma, nuclear atypia score 1,

Table 5. SUV cutoff and 10-year prognosis simulated by the software program Adjuvant!

Cutoff SUV	Category	Number of patients with IDC (136)	10-year prognisis by Adjuvant! (% ± SD)					
			Recurrence	*t* value	*P* value	Mortality	*t* value	*P* value
2	Low SUV group	37	27.6 ± 18.6	−3.88	0.0002	11.9 ± 18.1	−3.59	0.0005
	High SUV group	99	44.2 ± 23.3			26.9 ± 22.9		
3	Low SUV group	54	29.4 ± 20.3	−4.48	<0.0001	13.3 ± 19.4	−4.2	<0.0001
	High SUV group	82	46.5 ± 22.7			29.1 ± 22.7		
3.5	Low SUV group	62	29.4 ± 19.2	−5.14	<0.0001	13.3 ± 18.3	−4.85	<0.0001
	High SUV group	74	48.4 ± 23.1			30.9 ± 23.0		
4	Low SUV group	65	29.5 ± 18.2	−5.99	<0.0001	13.4 ± 17.4	−5.67	<0.0001
	High SUV group	71	51.0 ± 23.2			33.3 ± 23.4		
4.5	Low SUV group	63	29.1 ± 17.8	−5.56	<0.0001	13.0 ± 17.1	−5.14	<0.0001
	High SUV group	73	52.1 ± 22.9			34.4 ± 23.2		
5	Low SUV group	56	32.2 ± 20.0	−4.9	<0.0001	15.5 ± 18.6	−4.88	<0.0001
	High SUV group	80	50.6 ± 23.4			33.5 ± 24.1		

Table 6. Tumor characteristics in the cases that showed discrepancy between SUV and prognosis simulated by the software program Adjuvant!

No.	Age	SUV	Tumor size (cm)	Tumor invasive size (cm)	Grade	ER/PgR	HER2	Axillary FDG uptake	Number of axillary involvement	Relapse (%)	Mortality (%)
L1	40	2.14	1.6	1.6	3	+/+	1+	+	15	89	70
L2	54	2.82	5	5	2	+/−	1+	+	1	68	45
L3	48	2.6	4.5	2.5	3	+/+	2+	−	1(micro)	58	35
L4	41	2.73	12	12	2	+/+	0	+	18	93	77
H1	47	4.42	1.7	1.7	1	+/+	1+	−	0	18	3
H2	67	5.29	3.5	1.1	1	+/−	1+	−	0	18	3
H3	42	5.49	1.5	1.5	2	+/+	1+	−	0	25	8
H4	47	5.56	1	1	1	+/+	1+	−	0	18	3
H5	80	5.89	1.9	1.4	2	+/+	1+	−	0	25	8
H6	62	6.48	2	0.2	1	+/+	1+	−	0	18	3
H7	39	6.92	9.2	0.2	1	+/+	2+	−	0	15	1
H8	71	14.7	2.9	2.9	1	+/−	1+	−	0	26	9

micro, mircometastasis; FDG, fluorodeoxyglucose.

mitotic count score 1 and no nodal metastasis. Although other groups stratified by ER, PgR or c-erbB-2 might show significant differences, the mean levels of SUV in all groups were higher than 4.0.

Using a multivariate analysis, we showed bigger tumor invasive size, higher nuclear grade and ER negativity were independent variables correlated with high SUV in patients having primary breast cancer. The correlation coefficient of $R^2 = 0.72$ indicated 72% of tumoral SUV was explained by bigger tumor invasive size, higher nuclear grade and ER negativity. Likewise, in 78 patients having tumors 2 cm or less in size, 70% of tumoral SUV was explained by nuclear grade of primary breast cancer.

Some data of correlation between the level of SUV and clinicopathological parameters were published with regard to ^{18}F-FDG PET (5,6,13,14). In the present study, with regard to ^{18}F-FDG PET/CT, the results were similar, and the parameters for proliferative activities and aggressiveness of cancer cells were strongly correlated with high levels of SUV in cancer cells. We suppose that the levels of the SUV from ^{18}F-FDG uptake might be useful to predict biologically aggressive carcinoma cells.

The levels of SUV in IDC were significantly higher than that in ILC, as previously reported by other authors (5). And tumor grade was also a significant factor with a major influence on the level of SUV in breast cancer (14). Bos *et al.* described a significant correlation between ^{18}F-FDG uptake and mitotic activity of tumor cells (13). In contrast, Andreas *et al.* found there were no correlation of the level of ^{18}F-FDG uptake in primary breast cancers with tumor size, hormone receptors status, c-erbB-2 status or axillary lymph node involvement (6). Some parameters in the present report were inconsistent with the results described in the previous reports. Differences in criteria for judgment of positive and negative groups for c-erbB-2, hormone receptors, or those for categorization of nodal status and tumor size might have given rise to such inconsistency.

Some authors indicated that high levels of ^{18}F-FDG uptake are a prognostic factor for recurrence in patients having primary cancer (1,15,16). In the present study, we suggested the patients' group with a high SUV level might predict poor outcome in relapse and mortality by simulation using computed program Adjuvant! (Fig. 2). We considered that the SUV of 4.0 might be one of the optimal ones to predict prognosis. Ohtsuka *et al.* studied the prognostic significance of SUV on ^{18}F-FDG PET in patients with lung adenocarcinoma at pathological Stage I. They described that patients with tumor with 3.3 or higher of SUV showed higher rate of recurrence compared with patients with tumor with lower than 3.3 of SUV (17). The cutoff value of SUV 3.3 was similar with the value set in the present study.

As shown in Table 6, there were 12 patients with tumors with substantial discrepancy between the level of SUV in primary cancer and estimated prognosis. In four patients categorized as the low SUV group, the combination of other clinicopathological parameters by the computed program Adjuvant! indicated poor prognosis. In tumors of these four cases, three patients of the low SUV group, high level of SUV in axilla was detected by ^{18}F-FDG PET/CT and these findings could predict axillary lymph node metastasis. One remaining patient had solitary micrometastasis in an axillary sentinel node, but we could not pre-surgically detect a high level of SUV in axilla. Micrometastasis in the sentinel node was intraoperatively identified by frozen sectioning procedure. From the present results, we suppose that it might be difficult to predict metastatic potential to axillary lymph nodes by the level of SUV in primary cancer.

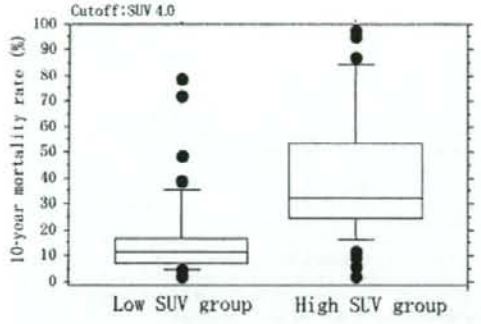

Figure 2. Prognostic significance of SUV simulated by the data published on computed program Adjuvant! (http://www.adjuvantonline.com). Mann–Whitney *U*-test reveals significant higher incidence of mortality after 10 years in high SUV (higher than 4.0) group compared to in low SUV (4.0 or less) group. Mean mortality rate (13.4% in low SUV group and 33.3% in high SUV group) are indicated with horizontal bars. The vertical bars indicate the range and the horizontal boundaries of the boxes represent 10 and 90% confidential indexes. Round plots represent outliers.

On the other hand, in eight patients with tumors categorized as the high SUV group, the combination of other clinicopathological parameters indicated better prognosis. All these eight patients were negative of axillary lymph node metastasis and had comparatively small sizes of tumor invasion (averaged 1.3 cm). One of the eight patients had a large sized tumor (9.2 cm in diameter), but the tumor was predominantly composed of an intraductal component, and the size of tumor invasion was only 0.2 cm in diameter. The histological types of these eight primary tumors were confirmed to be solid-tubular or papillotubular carcinoma, which were characterized by large nest, expansive growth of cancer cells and a smaller amount of stromal tissue component (data not presented).

From these results, it appeared that high density of viable cancer cells, regardless of invasive type or intraductal type, might contribute to high SUV levels of primary cancer.

Recently, primary systemic therapy has come to be widely performed for patients with early-stage breast cancer. CNB of tumor tissue becomes more important to know tumor characteristics before surgery. Many authors reported increased tumoral uptake of ^{18}F-FDG in breast cancer is closely correlated with the density of viable carcinoma cells, microvessel density and proliferative activity (4,5,18). These reports suggest that glucose hypermetabolism detected by ^{18}F-FDG using PET would reflect the dense proliferation of highly malignant breast cancer cells. Recently, ^{18}F-FDG PET/CT is more widely used than ^{18}F-FDG PET alone. The diagnostic accuracy of ^{18}F-FDG PET/CT is superior to that of CT or ^{18}F-FDG PET alone in the staging of patients with various cancers (19,20). Before primary systemic therapy, it might be possible to predict more precisely biological characteristics of primary breast cancer as well as the staging by the combination of ^{18}F-FDG PET/CT and CNB.

It is especially noteworthy that nuclear grade alone accounted for level of SUV for patients having tumor size 2 cm or less in a multiple regression analysis. This finding might prompt us to do further research for applying ^{18}F-FDG uptake in regarding an indication of primary systemic therapy of patients having early breast cancer treatment.

In conclusion, we showed significant correlation of the level of SUV in breast cancer with clinicopathological parameters and suggested its prognostic implications. It could be a useful tool to pretherapeutically predict biological characteristics and baseline risk of breast cancer.

Funding

This work was supported by a Grant-in-Aid for Promotion of Defense Medicine from the Ministry of Defense of Japan.

Conflict of interest statement

None declared.

References

1. Vansteenkiste JF, Stroobants SG, Dupont PJ, De Leyn PR, Verbeken EK, Deneffe GJ, et al. Prognostic importance of the standardized uptake value on (18)F-fluoro-2-deoxy-glucose-positron emission tomography scan in non-small-cell lung cancer: An analysis of 125 cases. Leuven Lung Cancer Group. *J Clin Oncol* 1999;17(10):3201–6.
2. Santiago JF, Gonen M, Yeung H, Macapinlac H, Larson S. A retrospective analysis of the impact of 18F-FDG PET scans on clinical management of 133 breast cancer patients. *Q J Nucl Med Mol Imaging* 2006;50(1):61–7.
3. Port ER, Yeung H, Gonen M, Liberman L, Caravelli J, Borgen P, et al. 18F-2-fluoro-2-deoxy-D-glucose positron emission tomography scanning affects surgical management in selected patients with high-risk, operable breast carcinoma. *Ann Surg Oncol* 2006;13(5):677–84.
4. Juweid ME, Cheson BD. Positron-emission tomography and assessment of cancer therapy. *N Engl J Med* 2006;354(5):496–507.
5. Buck AK, Schirrmeister H, Mattfeldt T, Reske SN. Biological characterisation of breast cancer by means of PET. *Eur J Nucl Med Mol Imaging* 2004;31(Suppl 1):S80–7.
6. Buck A, Schirrmeister H, Kuhn T, Shen C, Kalker T, Kotzerke J, et al. FDG uptake in breast cancer: correlation with biological and clinical prognostic parameters. *Eur J Nucl Med Mol Imaging* 2002;29(10):1317–23.
7. Smith TA, Sharma RI, Thompson AM, Paulin FE. Tumor 18F-FDG incorporation is enhanced by attenuation of P53 function in breast cancer cells in vitro. *J Nucl Med* 2006;47(9):1525–30.
8. Tatsumi M, Cohade C, Mourtzikos KA, Fishman EK, Wahl RL. Initial experience with FDG-PET/CT in the evaluation of breast cancer. *Eur J Nucl Med Mol Imaging* 2006;33(3):254–62.
9. Sato K, Tamaki K, Shigekawa T, Tsuda H, Kosuda S, Kusano S, et al. Clinically useful detection criteria for sentinel nodes in patients with breast cancer using a radioisotope technique. *Jpn J Clin Oncol* 2002;32(10):403–6.
10. Tsuda H, Tani Y, Weisenberger J, Kitada S, Hasegawa T, Murata T, et al. Frequent KIT and epidermal growth factor receptor overexpressions in undifferentiated-type breast carcinomas with 'stem-cell-like' features. *Cancer Sci* 2005;96(6):333–9.
11. Elston CW, Ellis IO. Pathological prognostic factors in breast cancer. I. The value of histological grade in breast cancer: experience from a large study with long-term follow-up. *Histopathology* 1991;19:403–10; *Histopathology* 2002;41(3A):151.
12. Ravdin PM, Siminoff LA, Davis GJ, Mercer MB, Hewlett J, Gerson N, et al. Computer program to assist in making decisions about adjuvant

therapy for women with early breast cancer. *J Clin Oncol* 2001;19(4):980–91.
13. Bos R, van Der Hoeven JJ, van Der Wall E, van Der Groep P, van Diest PJ, Comans EF, et al. Biologic correlates of (18)fluorodeoxyglucose uptake in human breast cancer measured by positron emission tomography. *J Clin Oncol* 2002;20(2):379–87.
14. Crippa F, Seregni E, Agresti R, Chiesa C, Pascali C, Bogni A, et al. Association between [18F]fluorodeoxyglucose uptake and postoperative histopathology, hormone receptor status, thymidine labelling index and p53 in primary breast cancer: a preliminary observation. *Eur J Nucl Med* 1998;25(10):1429–34.
15. Oshida M, Uno K, Suzuki M, Nagashima T, Hashimoto H, Yagata H, et al. Predicting the prognoses of breast carcinoma patients with positron emission tomography using 2-deoxy-2-fluoro[18F]-D-glucose. *Cancer* 1998;82(11):2227–34.
16. Higashi K, Ueda Y, Arisaka Y, Sakuma T, Nambu Y, Oguchi M, et al. 18F-FDG uptake as a biologic prognostic factor for recurrence in patients with surgically resected non-small cell lung cancer. *J Nucl Med* 2002;43(1):39–45.
17. Ohtsuka T, Nomori H, Watanabe K, Kaji M, Naruke T, Suemasu K, et al. Prognostic significance of [(18)F]fluorodeoxyglucose uptake on positron emission tomography in patients with pathologic stage I lung adenocarcinoma. *Cancer* 2006;107(10):2468–73.
18. Guo J, Higashi K, Ueda Y, Oguchi M, Takegami T, Toga H, et al. Microvessel density: correlation with 18F-FDG uptake and prognostic impact in lung adenocarcinomas. *J Nucl Med* 2006;47(3):419–25.
19. Chen YK, Su CT, Ding HJ, Chi KH, Liang JA, Shen YY, et al. Clinical usefulness of fused PET/CT compared with PET alone or CT alone in nasopharyngeal carcinoma patients. *Anticancer Res* 2006;26(2B):1471–7.
20. Antoch G, Saoudi N, Kuehl H, Dahmen G, Mueller SP, Beyer T, et al. Accuracy of whole-body dual-modality fluorine-18-2-fluoro-2-deoxy-D-glucose positron emission tomography and computed tomography (FDG-PET/CT) for tumor staging in solid tumors: comparison with CT and PET. *J Clin Oncol* 2004;22(21):4357–68.

BMC Cancer

BioMed Central

Research article

Open Access

Utility of ^{18}F-fluoro-deoxyglucose emission tomography/computed tomography fusion imaging (^{18}F-FDG PET/CT) in combination with ultrasonography for axillary staging in primary breast cancer

Shigeto Ueda[1], Hitoshi Tsuda*[2], Hideki Asakawa[1], Jiro Omata[1], Kazuhiko Fukatsu[3], Nobuo Kondo[4], Tadaharu Kondo[5], Yukihiro Hama[6], Katsumi Tamura[6], Jiro Ishida[6], Yoshiyuki Abe[6] and Hidetaka Mochizuki[1]

Address: [1]Department of Surgery, National Defense Medical College, 3-2 Namiki, Tokorozawa, Saitama 359-8513, Japan, [2]Department of Basic Pathology, National Defense Medical College, 3-2 Namiki, Tokorozawa, Saitama 359-8513, Japan, [3]Department of Basic Traumatology, National Defense Medical College, 3-2 Namiki, Tokorozawa, Saitama 359-8513, Japan, [4]Department of Oral Biochemistry, Ashahi University School of Dentistry, 1851 Hozumi, Mizuho, Gifu, 501-0296, Japan, [5]Section of Radiology, National Defense Medical College Hospital, 3-2 Namiki, Tokorozawa, Saitama 359-8513, Japan and [6]Tokorozawa PET Diagnostic Imaging Clinic, 7-5 Higashi-Sumiyoshi, Tokorozawa, Saitama 359-1124, Japan

Email: Shigeto Ueda - syueda2000@yahoo.co.jp; Hitoshi Tsuda* - htsuda@ndmc.ac.jp; Hideki Asakawa - hiddie_vr4@hotmail.com; Jiro Omata - dr20008@ndmc.ac.jp; Kazuhiko Fukatsu - kfukatsu@ndmc.ac.jp; Nobuo Kondo - nkondo@ndmc.ac.jp; Tadaharu Kondo - kondo@ndmc.ac.jp; Yukihiro Hama - yjhama2005@yahoo.co.jp; Katsumi Tamura - abe@toko-pet.or.jp; Jiro Ishida - abe@toko-pet.or.jp; Yoshiyuki Abe - abe@toko-pet.or.jp; Hidetaka Mochizuki - mochizuki@ndmc.ac.jp

* Corresponding author

Published: 9 June 2008

BMC Cancer 2008, 8:165 doi:10.1186/1471-2407-8-165

Received: 25 December 2007
Accepted: 9 June 2008

This article is available from: http://www.biomedcentral.com/1471-2407/8/165

Abstract

Background: Accurate evaluation of axillary lymph node (ALN) involvement is mandatory before treatment of primary breast cancer. The aim of this study is to compare preoperative diagnostic accuracy between positron emission tomography/computed tomography with ^{18}F-fluorodeoxyglucose (^{18}F-FDG PET/CT) and axillary ultrasonography (AUS) for detecting ALN metastasis in patients having operable breast cancer, and to assess the clinical management of axillary ^{18}F-FDG PET/CT for therapeutic indication of sentinel node biopsy (SNB) and preoperative systemic chemotherapy (PSC).

Methods: One hundred eighty-three patients with primary operable breast cancer were recruited. All patients underwent ^{18}F-FDG PET/CT and AUS followed by SNB and/or ALN dissection (ALND). Using ^{18}F-FDG PET/CT, we studied both a visual assessment of ^{18}F-FDG uptake and standardized uptake value (SUV) for axillary staging.

Results: In a visual assessment of ^{18}F-FDG PET/CT, the diagnostic accuracy of ALN metastasis was 83% with 58% in sensitivity and 95% in specificity, and when cut-off point of SUV was set at 1.8, sensitivity, specificity, and accuracy were 36, 100, and 79%, respectively. On the other hand, the diagnostic accuracy of AUS was 85% with 54% in sensitivity and 99% in specificity. By the combination of ^{18}F-FDG PET/CT and AUS to the axilla, the sensitivity, specificity, and accuracy were 64, 94, and 85%, respectively. If either ^{18}F-FDG PET uptake or AUS was positive in allixa, the probability of axillary metastasis was high; 50% (6 of 12) in ^{18}F-FDG PET uptake only, 80% (4 of 5) in AUS positive only, and 100% (28 of 28) in dual positive. By the combination of AUS and ^{18}F-FDG

PET/CT, candidates of SNB were more appropriately selected. The axillary ^{18}F-FDG uptake was correlated with the maximum size and nuclear grade of metastatic foci ($p = 0.006$ and $p = 0.03$).

Conclusion: The diagnostic accuracy of ^{18}F-FDG PET/CT was shown to be nearly equal to ultrasound, and considering their limited sensitivities, the high radiation exposure by ^{18}F-FDG PET/CT and also costs of the examination, it is likely that AUS will be more cost-effective in detecting massive axillary tumor burden. However, when we cannot judge the axillary staging using AUS alone, metabolic approach of ^{18}F-FDG PET/CT for axillary staging would enable us a much more confident diagnosis.

Background

Axillary lymph node (ALN) status is an important predictor regarding recurrence and survival of patients having primary breast cancer. Recently, sentinel node biopsy (SNB) has been introduced as a minimally invasive procedure to evaluate ALN status [1].

Accurate evaluation of ALN involvement is mandatory before treatment of primary breast cancer by following reasons; (1) ALN status is related to staging of disease and patients prognosis. (2) SNB can be beneficial for the patients to whom the presence of ALN involvement is not preoperatively detectable. They can avoid ALN dissection (ALND) when metastatic foci in sentinel nodes (SNs) are absent. (3) The status of ALN might influence on the decision of primary systemic chemotherapy (PSC). Patients with involved ALNs can be a candidate for PSC.

In our institute, we have carried out the identification of SNs using tin-colloid radioisotope technique [2]. SNs cannot be detected in patients having a massive ALN involvement because of poor uptake of radiotracer in SNs mostly replaced by tumor. Therefore, clinically node-positive patients are not candidates for SNB. Axillary ultrasonography (AUS) has been the most easy-applicable imaging tool for clinical staging of ALN status in patients having primary breast cancer [3,4].

We have used AUS to identify breast cancer patients who were eligible for optimal SNB [5]. Although AUS is not complete for the accurate determination of axillary nodal status, this tool is particularly sensitive for selecting patients with massive tumor burden. Actually, in a series of patients who were judged as candidates for SNB by AUS only, we reported that diagnostic accuracy of ALN status could be achieved 98.6%[5]. Positron emission tomography with ^{18}F-fluorodeoxyglucose (^{18}F-FDG PET) is expected to be a non-invasive approach to evaluate patients having ALN involvement. Recent studies using ^{18}F-FDG PET alone have shown low sensitivity, acceptable specificity, and acceptable positive predictive values in detection of ALN involvement [6-9]. In a prospective multicenter study in the U.S.A, diagnostic performance of ^{18}F-FDG PET in axillary staging showed relatively low sensitivity (mean 61%, ranging from 54% to 67%), and high specificity (mean 80%, ranging from 79 to 81%), when abnormal axillary focus was considered positive. In the same study, the ^{18}F-FDG PET in axillary staging had a lower sensitivity of 32% and a higher positive predictive value of 90%, when the cut-off of standerd uptake value (SUV) 1.8 or greater [10]. Veronesi et al also reported that the sensitivity of ^{18}F-FDG PET for detecting ALN involvement was 37%, but specificity and positive predictive value were 96% and 88%, respectively, at the threshold of SUV 1.2 [11].

Recently, fusion imaging systems combining ^{18}F-FDG PET and computed tomography (^{18}F-FDG PET/CT) have come to be applied in breast oncology. ^{18}F-FDG PET/CT can visualize anatomical location of the hypermetabolic cancer lesions better than ^{18}F-FDG PET or CT alone [12,13]. Therefore, the application of ^{18}F-FDG PET/CT might be very informative for detecting both regional lymph node involvement and distant metastasis.

We studied both a visual assessment of ^{18}F-FDG uptake and SUV for axillary staging, and compared the diagnostic accuracy between preoperative ^{18}F-FDG PET/CT and preoperative ultrasound in detecting ALN metastasis. We discussed the clinical management of the combonation of axillary ^{18}F-FDG PET/CT and AUS for the selection of proper candidates of SNB and PSC.

Methods

Patients

The study was done in accordance with the ethical principles of the Declaration of Helsinki and was approved by the institutional review board in the National Defense Medical College (NDMC). Informed consents were obtained from all patients with regard to ^{18}F-FDG PET/CT examination and the entry into the present study.

This prospective study enrolled a series of 183 patients having primary breast cancer proven by core needle biopsy at the National Defense Medical College Hospital from April 2005 through August 2007. For axillary staging, all patients underwent both ^{18}F-FDG PET/CT and ultrasonography within 5 weeks before surgery. Patients

with diabetes mellitus or pregnancy, those who underwent primary systemic therapy, those who underwent excisional biopsy were excluded. During the entry period, we experienced 15 patients who were diagnosed by ^{18}F-FDG PET/CT to have breast cancer with distant metastases, comprising four distant lymph node metastases, nine bone metastases, and two lung metastases. Patients having distant metastases were also ineligible for this study.

Axillary ultrasound examination

AUS was performed using ProsoundII SSD 6500 (Aloka, Tokyo, Japan) employing a 10-MHz linear array transducer. AUS criteria in our institute were described previously [5]. In brief, homogeneously hypoechoic lymph nodes with diameters of 10 mm or more and in oval or round shape were defined as AUS-positive and were considered to be potentially extensive nodal involvement. Lymph nodes with central hyperechoic area and/or with diameter of less than 10 mm, defined as AUS-negative were considered to be clinically node-negative. One experienced ultrasonographer (T.K) performed axillary examination of operable patients. At least two breast surgeons discussed and determined AUS status together with the ultrasonographer in weekly conference.

Surgery and Sentinel node biopsy procedure

The 183 patients underwent mastectomy or breast-conserving surgery with SNB and/or ALND. SNB was performed using the procedure described previously [2]. According to SNB protocol in our institute, patients having AUS negativity were eligible for SNB and were optionally performed SNB after the acquisition of informed consent. For patients having AUS positivity or those who rejected SNB, ALND was performed.

SNs were intraoperatively examined histopathologically. Biopsied SNs were cut into 2-mm-thick slices, and histopathological sections were made from each slice. These sections were stained with hematoxylin and eosin, and at least two pathologists examined the sections. All patients having SN metastasis recieved ALND. If SNs were free of cancer cells, ALND was omitted.

^{18}F-FDG PET/CT and quantification of ^{18}F-FDG uptake in axilla

All patients received ^{18}F-FDG PET/CT scans (Biograph LSO Emotion, 3D model, Siemens, Germany) at Tokorozawa PET Diagnostic Imaging Clinic (Tokorozawa, Japan). Blood glucose level was measured in each patient and did not exceed 120 mg/dl.

Patients fasted at least 4 hours before ^{18}F-FDG PET study. One hour after intravenous administration of 3.7 Mbq/kg ^{18}F-FDG, a transmission scan using CT (SOMATO Emotion, 16-slice configuration, pitch 1.83, Siemens, Germany) for attenuation correction and anatomical imaging was acquired for 90 sec. IV contrast was not administered to patients for the CT portion of the ^{18}F-FDG PET/CT.

Back projection image was obtained after Gaussian filter was applied. The spatial resolution of the reconstructed images was 6.0–7.0 mm in cranio-caudal, 6.3–7.1 mm in right-left and 6.3–7.1 mm in anterior-posterior directions.

A regions of interest (ROI) was placed in the axillary lesion, including the highest uptake area (circle ROI, 2 cm in diameter), and SUV maximum in the ROI was calculated. The SUV was decay-corrected tissue activity divided by the injected dose per patient body, and was calculated using the following formula: SUV = activity in region of interest/decay factor of F-18 (MBq/ml)/injected dose (MBq/kg body weight).

CT images were also available for evaluation. Visual assessment of ^{18}F-FDG uptake was carried out by at least two experienced nuclear medicine radiologists, and abnormal axillary uptake greater than background activity was interpreted as suspicious nodal involvement. Semi-quantitative measurement of SUV was done on any axillary focus with abnormal uptake.

Determination of the optimal SUV cut-off points

To determine the optimal SUV cut-off point, the tentative SUV cut-off point was established, ranging from 0.8 to 3.0 with 0.2 to 0.3 increments. SUV of the cut-off point or greater was defined as positive and SUV less than the point was defined as negative. The SUV of 0.4 is the lowest limit of visible uptake of ^{18}F-FDG. Based on each SUV cut-off point, the diagnostic accuracy of ^{18}F-FDG PET/CT (positive or negative) was evaluated by means of sensitivity, specificity, positive predictive value (PPV), and negative predictive value (NPV).

Histopathological study

The number, the maximum size, and nuclear grade of involved ALNs were histopathologically examined.

Statistical analysis

Statistical analysis was performed using Statview 5.0 version (SAS Institute Inc). As univariate analysis, Mann-Whitney *U* test and chi square test were used to establish the correlation between clinicopathological variables and axillary SUV. *P* value of 0.05 or less was defined as statistical significance.

Results

Patient characteristics

Patient age, pathological T factor, histological type, nuclear grade, hormonal receptor status and c-erbB2 sta-

Table 1: Patient characteristics

Variables		Number 183	% 100
Age	mean [range]	57 [32–81]	
	<45	33	18
	45 ≦	150	82
pT-stage	pTis	10	5
	pT1	91	50
	pT2	68	37
	pT3	14	8
Histology	DCIS	9	5
	IDC	158	86
	ILC	9	5
	Apocrine	2	1
	Mucinous	2	1
	Squamoid	1	1
	Paget	2	1
Nuclear grade	1	59	32
	2	51	28
	3	69	38
	Not graded	4	2
Nodal metastasis	negative	124	68
	positive	59	32
Estrogen receptor (ER)	10%>	44	24
	10% ≦	139	76
Progesterone receptor(PgR)	10%>	63	34
	10% ≦	120	66
c-erbB-2 (HER2)	0 to 2+	152	83
	3+/FISH Amp	28	15
	unknown	3	2
Primary axillary approach	Ax dissection	58	32
	SNB	125	68
SUV of the primary tumor	mean [range]	4.3 [0.9–17.8]	
SUV of axillary uptake*	mean [range]	3.0 [0.4–11.3]	

DCIS, ductal carcinoma in situ; IDC, invasive ductal carcinoma; ILC, invasive lobular carcinoma; Mucinous, mucinous carcinoma; Apocrine, apocrine carcinoma; Squamoind, Squamoid carcinoma; Paget, Paget's disease; FISH Amp, FISH Amplication; Ax, axillary; SNB, sentinel node biopsy; SUV, Standardized Uptake Value; *Visible uptake of 18F-FDG

tus of the primary tumors, and SUV of the primary tumors and axillary uptake are listed in Table 1, ALN involvement was histopathologically detected in 59 (32%) of 183 patients.

The mean SUV of the primary tumor in the 183 patients was 4.3, ranging from 0.9 to 17.8, and the mean SUV of the axilla was 3, ranging 0.4 to 11.3. The SUVs of 0.4 and 11.3 were the lowest point and the highest point to visualize ^{18}F-FDG uptake, respectively. The mean interval between ^{18}F-FDG PET/CT and surgery was 29 days. One hundred twenty-five (68%) of the 183 patients underwent initial SNB. One hundred twenty-four (99%) of the 125 patients were successfully performed SNB. The number of removed SNs per patient was 2.4 on an average. Metastases to SNs were positive in 24 (19%) patients, and all of these patients underwent ALND. Metastases to the SNs were negative in 100 (81%) patients, and none of them recieved further axillary surgery. Other 58 (32%) patients underwent ALND without SNB.

Diagnostic performance of ^{18}F-FDG PET/CT and ultrasonography in axillary staging

Diagnostic performance for detecting axillary involvement was compared between ^{18}F-FDG PET/CT and ultrasonography (Table 2).

By visual assessment of ^{18}F-FDG PET/CT, axillary uptake was positive in 40 (22%) patients and negative in 143 (78%) patients. Of these 40 axillary-positive patients, 34 (85%) were truely positive, whereas 6 (15%) were false positive. Of the 143 axillary- negative patients, 118 (83%) patients were truely negative, whereas 25 (17%) patients were false negative. Sensitivity, specificity, PPV, NPV, and accuracy of visual assessment of ^{18}F-FDG PET/CT were 58, 95, 85, 83, and 83%, respectively.

Table 2: Diagnostic performance of ^{18}F-FDG PET/CT and ultrasonography in axillary staging

^{18}F-FDG uptake	TP	TN	FP	FN	Sensitivity (%)	Specificity (%)	PPV (%)	NPV (%)	Accuracy (%)
Visual assessment	34	118	6	25	57.6	95.2	85	82.5	83.1
SUV cutoff point									
0.8	30	118	6	29	50.8	95.2	83.3	80.3	80.9
1.3	24	122	2	35	40.7	98.4	92.3	77.7	79.8
1.5	21	123	1	38	35.6	99.2	95.5	76.4	78.7
1.8	21	124	0	38	35.6	100	100	76.5	79.2
2	20	124	0	39	33.9	100	100	76.1	78.7
3	16	124	0	43	27.1	100	100	74.3	76.5
AUS	32	123	1	27	54.2	99.2	97	82	84.7
Visual assessment of ^{18}F-FDG uptake Combined with AUS	38	117	7	21	64.4	94.4	84.4	84.8	84.7

AUS, Axillary ultrasonography; TP, True positive; TN, True negative; FP, False positive; FN, False negative; PPV, Positive predictive value; NPV, Negative Predictive value;

The accuracy of diagnosis of ^{18}F-FDG PET/CT was compared among various SUV cut-off points ranging from 0.8 to 3.0, using entire data set of 183 patients.

When a SUV cut-off points were set from 0.8 up to 1.8, specificity increased from 95% to 100%, but sensitivity decreased from 51% to 36%. As SUV increased over 1.8, specificity of 100% did not vary, but sensitivity further decreased. When the SUV was 1.8, PPV, NPV and accuracy were 100%, 77%, and 79%, respectively. Therefore, the SUV of 1.8 achieved excellent specificity and PPV, but low sensitivity in comparison with visual assessment.

Ultrasonography detected 33 (18%) AUS-positive patients and 150 (82%) AUS-negative patients. Of the 33 AUS-positive patients, thirty-two patients (97%) were truely positive, and one patient (3%) was false-positive. Of the 150 AUS-negative patients, 123 (82%) were truely negative, whereas 27 (18%) were false-negative. Sensitivity, specificity, PPV, NPV, and accuracy were 54, 99, 97, 82, and 85%, respectively.

Combined with visual assessment of ^{18}F-FDG uptake and AUS, 138 (75%) patients with double-negative ^{18}F-FDG uptake and AUS were considered to be nodal negative, and 45 (25%) patients with positive finding in the visual assessment of ^{18}F-FDG uptake and/or AUS were considered to be nodal positive. Sensitivity, specificity, PPV, NPV, and accuracy of the combination were 64, 94, 84, 85, and 85%, respectively.

Feasibility of SNB for patients having negative AUS

Of the 150 patients having negative AUS, 125 (83%) consented and underwent SNB. Table 3 shows diagnostic performance of SNB in axillary staging in AUS-negative patients. SNB identification rate was 99.2% (124 of 125 patients). Twenty five patients (20%) had axillary nodal metastasis in permanent pathology. Intraoperative pathological diagnosis of metastasis in SNB was accurately performed in 123 (99%) of 124 patients. One patient (1%) was false negative by frozen section intraoperatively, but a micrometastatic deposit was postoperatively detected in one of sentinel nodes by permanent histology. With regard to intraoperative pathological diagnosis of metastasis in SNB, sensitivity, specificity, PPV, NPV and overall accuracy were 96, 100, 100, 99, and 99% respectively in Table 3A.

In the 12 AUS-negative but ^{18}F-FDG uptake positive patients who consented and recieved SNB, 6 (50%) had ALN involvement. One (8%) patient was false negative. With regard to intraoperative pathological diagnosis of SLN, sensitivity, specificity, PPV, NPV, and overall accuracy were 83, 100, 100, 86, and 92%, respectively in Table 3B.

In the 112 AUS-negative and ^{18}F-FDG uptake negative patients, who consented and underwent SNB, 19 (17%) had ALN involvement. With regard to intraoperative pathological diagnosis of SNB, sensitivity, specificity, PPV, NPV, and overall accuracy were all 100% in Table 3C.

Axillary nodal clinicopathological factors correlated with ^{18}F-FDG uptake

Table 4 shows correlation of axillary ^{18}F-FDG uptake with nodal clinicopathological factors of 59 patients having ALN involvement. The maximum size and nuclear grade of involved ALN were significantly correlated with ^{18}F-FDG uptake at SUV cut-off point 1.8 ($p = 0.006$ and 0.03, respectively). The number of involved ALNs was not cor-